World Academy of Science, Engineering and Technology
International Journal of Nuclear and Quantum Engineering
Vol:5, No:6, 2011

Temperature Effect on the Mechanical Properties of Pd_3Rh and $PdRh_3$ Ordered Alloys

J. Davoodi , J. Moradi

***Abstract*—**The aim of this research was to calculate the mechanical properties of Pd_3Rh and $PdRh_3$ ordered alloys. The molecular dynamics (MD) simulation technique was used to obtain temperature dependence of the energy, the Yong modulus, the shear modulus, the bulk modulus, Poisson's ratio and the elastic stiffness constants at the isobaric-isothermal (NPT) ensemble in the range of 100-325 K. The interatomic potential energy and force on atoms were calculated by Quantum Sutton-Chen (Q-SC) many body potential. Our MD simulation results show the effect of temperature on the cohesive energy and mechanical properties of Pd3Rh as well as PdRh3 alloys. Our computed results show good agreement with the experimental results where they have been available.

***Keywords*—**Pd-Rh alloy; Mechanical properties; Molecular dynamics simulation

I. Introduction

THE Pd-based alloys have been studied for more than 100 years in both fundamental and application aspects. Especially, in the last three decade thermodynamic and mechanical properties of pd-based alloys were studied by molecular dynamics simulation technique [1-8]. Among the Pd-based alloys, the Pd-Rh alloy is of special interest owing to their increased hydrogen absorption capacity. Moreover, Pd-based alloys can potentially offer improvements to pure Pd membranes [9-20]. Very few experimental data are available for the mechanical properties of Pd_3Rh and $PdRh_3$ ordered alloys in the various temperatures. The phase-stability of PdRh alloys was studied by Tanusri Saha and Abhijit Mookerjee [19]. J. Luyten et al provided theoretical estimates for the heats of mixing of the binary systems Pt-Rh, Pt-Pd and Pd-Rh and the ternary Pt-Pd-Rh systems. The heats of mixing and the phase diagrams were calculated with Monte Carlo simulations and with the semi-empirical modified embedded atom method [13]. In the other investigation, M. Hara et al were investigated absorption and desorption isotherms of protium and deuterium were measured for pd-based alloys [20].

In this investigation, we have performed MD simulation under constant pressure, constant temperature conditions [21, 22] to calculate the mechanical properties including, Yong modulus, the shear modulus, the bulk modulus, Poisson's ratio and the elastic stiffness constants of Pd_3Rh and $PdRh_3$ ordered alloys. The Q-SC potential [5, 24] parameters of the pure Pd and Rh metals were used as interatomic potential parameters to calculate the cohesive energy as well as the mechanical properties of Pd, Rh pure metals and Pd_3Rh and $PdRh_3$ ordered alloys. We have calculated mechanical properties and cohesive energy of Pd, Rh elements under atmospheric pressure for evaluating computer codes and the interatomic potential.

J. Davoodi is with the University of Zanjan, Zanjan, Iran (phone: +982412353; fax: +982412283203; e-mail: jdavoodi@znu.ac.ir).
J. Moradi is with the University of Zanjan, Zanjan, Iran (phone: +982412353; fax: +982412283203).

II. Details of MD simulation

A. Interatomic potential

The force experienced by individual atom i in an N-atom cluster was obtained from Q-SC interatomic potential energy function. The potential energy of the pure metals and alloys in Sutton-Chen formalism for the systems of N atoms is given as follows [5, 24]

$$U_{tot} = \sum_{i=1}^{N}\left[\sum_{j\neq i}\varepsilon_{ij}\frac{1}{2}\left(\frac{a_{ij}}{r_{ij}}\right)^{n_{ij}} - c_i\varepsilon_{ii}\left(\sum_{j\neq i}\left(\frac{a_{ij}}{r_{ij}}\right)^{m_{ij}}\right)^{1/2}\right] \quad (1)$$

The first term in equation (1) is a two body interaction between the atoms i and j, the second term represents the many-body cohesion term associated with atom i, a is the length parameter scaling to the lattice spacing of the crystal, c is a dimensionless parameter scaling the attractive terms, ε is an energy parameter determined from experiment, and n, m are integer parameter with $n>m$ which determine the range of the two component of the potential (Table I).

TABLE I
THE Q-SC POTENTIAL PARAMETERS FOR PD-RH MODEL ALLOY SYSTEM

Interaction	*ε(eV)*	*a(Å)*	*c*	*n*	*m*
Pd-Pd	0.003286	3.8813	148.20	12	12
Rh-Rh	0.002461	3.7984	305.49	13	13
Pd-Rh	0.002843	3.8396	------	12.5	12.5

To construct the potential for the binary alloy state, Pd-Rh, from the corresponding Q-SC potentials for the elemental state, we used the following mixing rule [6, 9]

$$\varepsilon_{ij} = (\varepsilon_i\varepsilon_j)^{1/2}, \quad a_{ij} = (a_i a_j)^{1/2} \quad (2)$$

$$m_{ij} = \frac{(m_i + m_j)}{2}, \quad n_{ij} = \frac{(n_i + n_j)}{2} \quad (3)$$

B. Temperature and pressure control

The temperature control was implemented via the Nose-Hoover heat bath [25, 26] whose introduction modifies the

standard velocity Verlet equation of motion [22] to the following forms [27]

$$\vec{r}_i(t+\delta t)=\vec{r}_i(t)+\delta t\vec{v}_i(t)+\frac{1}{2}\delta t^2\left[\frac{\vec{f}_i(t)}{m_i}-\zeta(t)\vec{v}_i(t)\right]$$

$$\vec{v}_i(t+\frac{1}{2}\delta t)=\vec{v}_i(t)+\frac{\delta t}{2}\left[\frac{\vec{f}_i(t)}{m_i}-\zeta(t)\vec{v}_i(t)\right]$$

$$\zeta(t+\tfrac{1}{2}\delta t)=\zeta(t)+\frac{\delta t}{2Q}\left[\sum_i^N m_i\vec{v}_i^2(t)-gk_bT\right] \quad (4)$$

$$\zeta(t+\delta t)=\zeta(t+\tfrac{1}{2}\delta t)+\frac{\delta t}{2Q}\left[\sum_i^N m_i\vec{v}_i^2(t+\tfrac{1}{2}\delta t)-gk_bT\right]$$

$$\vec{v}_i(t+\delta t)=\frac{2}{2+\delta t\zeta(t+\delta t)}\left[\vec{v}_i(t+\tfrac{1}{2}\delta t)+\frac{1}{2}\delta t\frac{\vec{f}_i(t+\delta t)}{m_i}\right]$$

where ζ is the time-dependent friction of the heat bath. A particular parameterization of the Q is given by

$$Q=gk_bT\tau^2 \quad (5)$$

where τ is the relaxation time of the heat bath, normally of the same order of magnitude as the simulation time step. This parameter controls the speed with which the bath damps down the fluctuation in the temperature. The number of degrees of freedom is given by $g=3(N-1)$.

The standard Berendsen barostat [28] was used for pressure control of the system. The Berendsen barostat uses a scale factor, μ, which is a function of instantaneous pressure, P, to scale lengths in the system

$$\begin{aligned} x(i) &\rightarrow \mu x(i) \\ y(i) &\rightarrow \mu y(i) \\ z(i) &\rightarrow \mu z(i) \\ L &\rightarrow \mu L \end{aligned} \quad (6)$$

where μ is given by

$$\mu=\left[1+\frac{\delta t}{\tau_p}(P-P_0)\right]^{1/3} \quad (6)$$

Here, τ_p is the rise time of the barostat, and P_0 is the set point pressure. The system pressure is set toward a desired value by changing the dimensions of the simulation cell size during the simulation.

C. Simulation data

Our simulations were carried out using molecular dynamics beads on Q-SC interatomic potential energy function. The simulations involved clusters of Pd and Rh pure metals, and Pd_3Rh, $PdRh_3$ ordered alloys. The total number of atoms present was 2048 for both pure metals and alloys. The simulation time step was set to 0.5 *fs*. The periodic boundary conditions were employed in all directions. The clusters were first equilibrated for 10000 time steps at T=100 K, and then the temperature was raised by 1K at each temperature step. At each step that the temperature was increased, the system was re-equilibrated for 1000 time steps. Figs. 1 and 2 show the variation of energy, volume and pressure in order to obtain the equilibrium state. These quantities approached to constants values to make sure that the system had reached equilibrium as seen in figures.

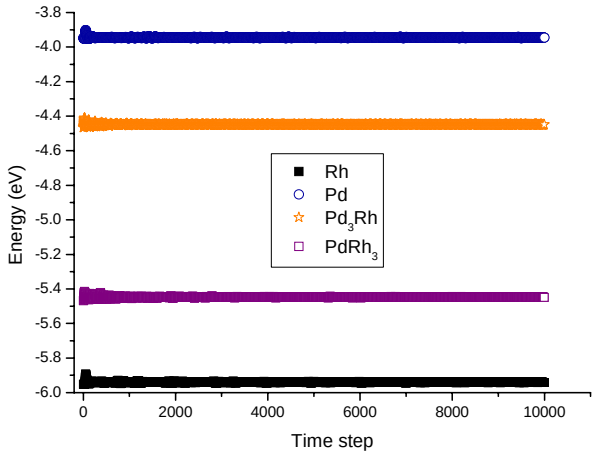

Fig. 1 Time variation of the cohesive energy for Pd, Rh, Pd_3Rh and $PdRh_3$ during equilibration phase

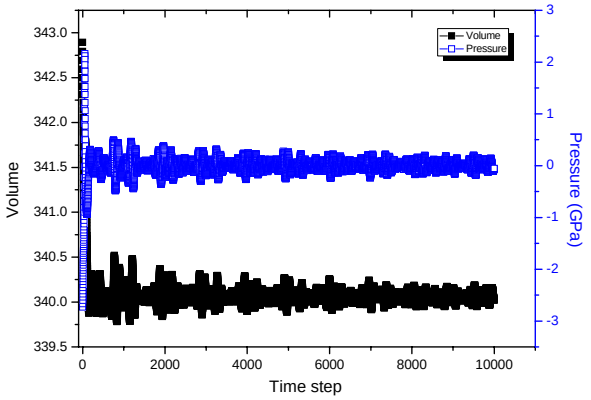

Fig. 2 Time variation of the volume and pressure for Pd_3Rh during equilibration phase

III. Results and Discussion

The quantities that were calculated in these MD simulations were the mechanical properties including the Yong modulus, the shear modulus, the bulk modulus, Poisson's ratio and the elastic stiffness constants of Pd, Rh, Pd_3Rh and $PdRh_3$. According to the hooke's law, for small deformation, the stress components σ_{ij} are directly proportional to the strain

components ε_{ij}. This relation can be expressed in mathematical terms as [29]

$$\sigma_{ij} = C_{ijkl}\varepsilon_{kl} \tag{8}$$

where C_{ijkl} are the elastic stiffness constants. The number of independent elastic stiffness constants is reduced if the crystal possesses symmetry elements. For example, for cubic crystal, there are only three independent constants (C_{11}, C_{12}, C_{44}) [29]. In terms of the interatomic potential, these constants can be expressed as [30]

$$c_{11} = \frac{1}{\mathrm{v}}\frac{\partial^2 E^{(1)}}{\partial \varepsilon_{11}^2}$$
$$c_{12} = \frac{1}{\mathrm{v}}\frac{\partial^2 E^{(1)}}{\partial \varepsilon_{11}\partial \varepsilon_{22}} \tag{9}$$
$$c_{44} = \frac{1}{4\mathrm{v}}\frac{\partial^2 E^{(1)}}{\partial \varepsilon_{12}^2}$$

where $E^{(1)}$ and v are the total energy of an atom and the volume per atom, respectively. We have used the Reuss assumption to estimate the bulk modulus B, shear modulus G, young modulus E, and Poisson's ratio v, according the following relations [31]

$$B = (c_{11} + 2c_{12})/3 \tag{10}$$
$$G = 5(C_{11} - C_{12})/(4C_{44} + 3(C_{11} - C_{12})) \tag{11}$$
$$E = 9GB/(3B + G) \tag{12}$$
$$v = (3B - 2G)/2(3B + G) \tag{13}$$

Figs. 3-10 show the temperature dependence of energy, elastic stiffness constants (C_{11}, C_{12}, C_{44}), Bulk modulus, shear modulus, Young modulus, and Poisson's ratio respectively.

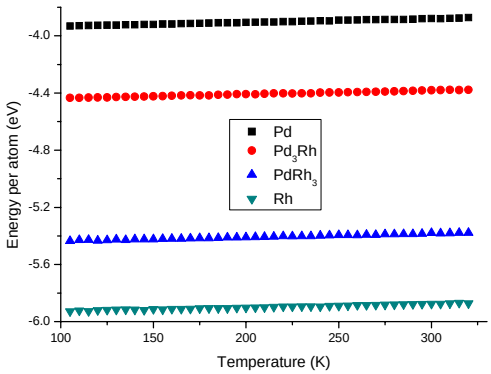

Fig. 3 Variation of energy of Pd, Rh, Pd_3Rh and $PdRh_3$ with temperature

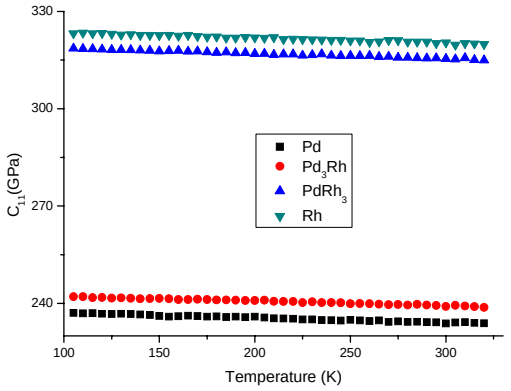

Fig. 4 Variation of elastic stiffness constant (C_{11}) of Pd, Rh, Pd_3Rh and $PdRh_3$ with temperature

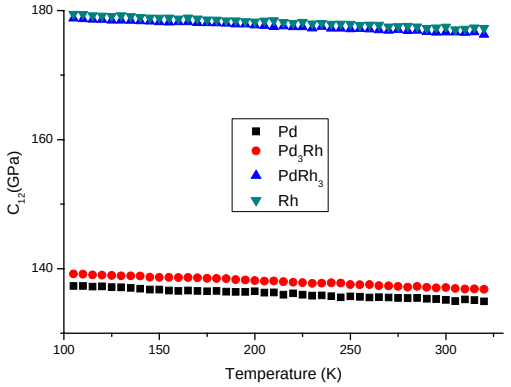

Fig. 5 Variation of elastic stiffness constant (C_{12}) of Pd, Rh, Pd_3Rh and $PdRh_3$ with temperature

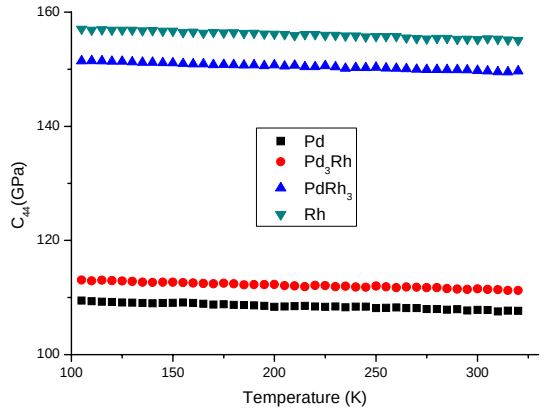

Fig. 6 Variation of elastic stiffness constant (C_{44}) of Pd, Rh, Pd_3Rh and $PdRh_3$ with temperature

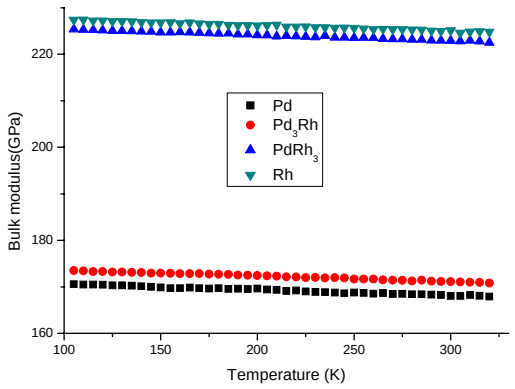

Fig. 7 Variation of Bulk modulus of Pd, Rh, Pd_3Rh and $PdRh_3$ with temperature

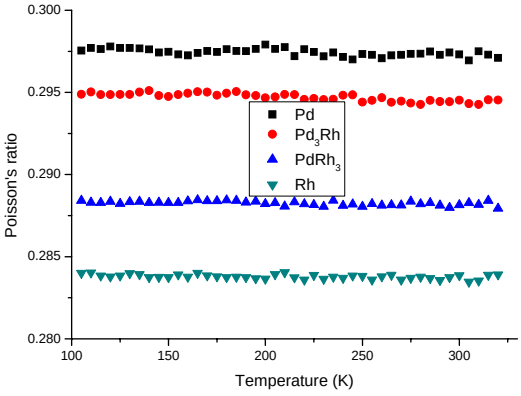

Fig. 10 Variation of Poisson's ratio of Pd, Rh, Pd_3Rh and $PdRh_3$ with temperature

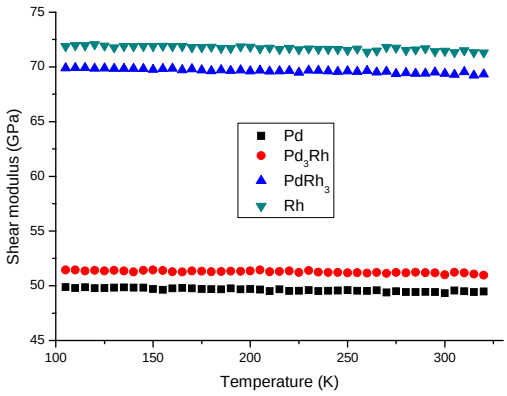

Fig. 8 Variation of shear modulus of Pd, Rh, Pd_3Rh and $PdRh_3$ with temperature

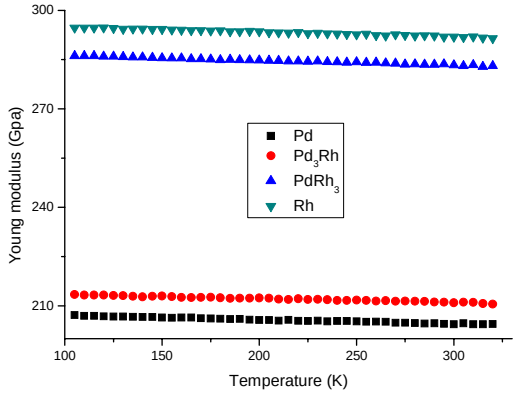

Fig. 9 Variation of Young modulus of Pd, Rh, Pd_3Rh and $PdRh_3$ with temperature

Our motivation for computing these properties for the elemental materials was to obtain an estimate of the accuracy of the Q-SC potentials. A comparison of the results for the elemental materials shows that our computed values are in reasonable agreement with the experimental data that are available for these materials. This can give an indication of the quality of the alloy potential energy functions that we have constructed on the basis of these elemental potentials. The percentage errors associated with the computed values, as compared to the experimental data are listed in Table II.

TABLE II
THE PERCENTAGE ERROR OF THE COMPUTED VALUES VIS-A-VIS THE EXPERIMENTAL DATA

Physical properties	Pd	Rh
Cohesive energy	0.2	0.8
C11	2.6	3.2
C12	16.2	5.7
C44	24.3	17.5
B	15.7	9.5
G	13.1	31.1
E	5.3	11.5
v	21.3	7.6

The variation of cohesive energy with temperature for both elemental materials Pd, Rh, and the ordered alloy Pd_3Rh and $PdRh_3$ were plotted in the fig. 3. We see that the energy of Pd, Rh , Pd_3Rh and $PdRh_3$ increase with temperature. This is particularly true for the variation of the energy with temperature.

The temperature dependence of the mechanical properties are shown in figures 4-10. From figures 4-9, we see that the elastic stiffness constants, the bulk modulus, the shear modulus and the Yong modulus decrease concurrent with the increased temperature. This decrease is essentially linear with temperature, and has agreement with an approximate equation describing the modulus-temperature relitionshipe according the following relation [32]

$$M = M_0\left[1 - a\left(\frac{T}{T_m}\right)\right] \quad (12)$$

where M is the modulus at temperature T and M_0 the modulus at 0K. The proportionality constant a for most crystal solids is on the order of 0.5. The results for the Poisson's ratio are shown in fig. 10. This fig. shows that the Poisson's ratio is approximately constant in the range of 100-325 K.

IV. Conclusion

In this paper, we have performed molecular dynamics simulations, based on Q-SC potential, to investigate the mechanical properties of pure Pd, Rh metals and Pd_3Rh, $PdRh_3$ ordered alloys. The temperature dependence of the energy, the elastic stiffness constants, the bulk modulus, the shear modulus, the Yong modulus and Poisson's ratio were obtained from these simulations. The results from our simulations show that our choice of the interatomic potential and the mixing rule employed to construct the alloy states lead to a good prediction of the properties of these materials. This research shows the cohesive energy increase with temperature. Moreover, the mechanical properties, except Poisson's ratio, decrease with the increased temperature in a linear manner. Also, the Poisson's ratio remains approximately constant in the range of 100-325 K.

References

[1] H. H. Kart, M. Tomak, M. Uludogan, et al, International journal of modern physics B. 18, 2004, pp. 2257-2269.
[2] S. Ozdemir Kart, M. Tomak, M. Uludogan, and T. Cagin, J. Noncryst. Sol. 337, 2004, pp. 101-108.
[3] H. H. Kart, M. Tomak, M. Uludogan, T. Cag?n, Turk. J. Phys. 30, 2006, pp. 311-317.
[4] J. Davoodi, M. Ahmadi, H. Rafii-Tabar, Material science and engineering A 527, 2010, pp. 4008-4013.
[5] H. H. Kart, M. Tomak, M. Uludogan, T. Cag?n, Comput. Mater. Sci. 32, 2005, pp. 107-117.
[6] J. Davoodi, M. Ahmadi, Computational materials science 49, 2010, pp. 21-24.
[7] S. Ozdemir Kart, M. Tomak, M. Uludogan, and T. Cagin, J. Noncryst. Sol. 337, 2004, pp. 101-108.
[8] H. H. Kart, M. Tomak, M. Uludogan, T. Cag?n, Materials science and engineering A-Structural materials properties microstructure and processing 435, 2006, pp. 736-744.
[9] J.C. Barton, J.A.S. Green, F.A. Lewis, Trans. Faraday Soc. 62, 1966, pp. 960.
[10] F.A. Lewis, W.D. McFall, T.C. Witherspoon, Z. Phys. Chem. N. F. 84, 1973, pp. 31.
[11] Y. Sakamoto, Y. Haraguchi, M. Ura, F.L. Chen, Ber. Bunsenges Phys. Chem. 98, 1994, pp. 964.
[12] Y. Sakamoto, K. Kuruma, Y. Naritomi, J. Appl. Electrochem. 24, 1994, pp. 38.
[13] J. Luyten, J. De Keyzer, P. Wollants, C. Creemers, CALPHAD: Computer Coupling of Phase Diagrams and Thermochemistry 33, 2009, pp. 370-376.
[14] B. Baranowski, S. Majchrzak, T.B. Flanagan, J. Phys. Chem. 77, 1973, pp. 35.
[15] Y. Sakamoto, F.L. Chen, M. Ura, T.B. Flanagan, Ber. Bunsenges Phys. Chem. 99, 1995, pp. 807.
[16] G. Mengoli, M. Fabrizio, C. Manduchi, E. Milli, G. Zannoni, J. Electroanal. Chem. 390, 1995, pp. 135.
[17] A.K.M. Fazle Kibria, T. Kubota, A. Kagawa, Y. Sakamoto, Int. J. Hydrogen Energy 24, 1999, pp. 747.
[18] A.K.M. Fazle Kibria, Y. Sakamoto, Int. J. Hydrogen Energy 25, 2000, pp. 853.
[19] T. Saha and A. Mookerjee, J. Phys.: Condens. Matter 9, 1997, pp. 2179–2186.
[20] M. Hara, L. Wan, M. Matsuyama, K. Watanabe, Journal of Alloys and Compounds 428, 2007, pp. 252–255.
[21] H. J. C. Berendsen, J. P. M. Postma, W. F. van Gunsteren, A. DiNola, and J. R. Haak, J. Chem. Phys. 81, 1984, pp. 3684-3690.
[22] J.M. Haile, Molecular Dynamics Simulation, John Wiley & Sons, New York, 1992.
[23] H. Rafii-Tabar, A. P. Sutton, Phil. Mag. Lett. 63, 1991, pp. 217-224.
[24] Y. Qi, T. Cag?n, Y. Kimura and W.A. Goddard, Phys. Rev. B 59, 1999, pp. 3527-3533.
[25] W. G. Hoover, Canonical dynamics: Phys. Rev. A 31, 1985, pp. 1695-1697.
[26] S. Nose, J. Chem. Phys. 81, 1984, pp. 511-519.
[27] A.P. Sutton, J.B. Pethica, H. Rafii-Tabar, J.A. Nieminen, in: D.G. Pettifor, A.H. Cottrell (Eds.), Electron Theory in Alloy Design, Institute of Materials, London, 1994, 191.
[28] H. J. C. Berendsen, J. P. M. Postma, W. F. van Gunsteren, A. DiNola, and J. R. Haak, J. Chem. Phys. 81, 1984, pp. 3684-3690.
[29] C. Kittel, Introduction to Solid State Physics, eighth ed., John Wiley & Sons, New York, 2005.
[30] A. P. Sutton and J. Chen, Phil. Mag. Lett. 61, 1990, pp. 139-164.
[31] J.F. Nye, Propriétés Physiques des Matériaux, Dunod, 1961.
[32] T.H. Courtney, Mechanical behavior of metals, second ed., McGraw-Hill, New York, 2000.